Physical and Mechanical Behavior of Sterilized Biomedical Segmented Polyurethanes

G. A. ABRAHAM, P. M. FRONTINI, T. R. CUADRADO

Institute of Materials Science and Technology (INTEMA), National University of Mar del Plata–National Research Council (CONICET), J. B. Justo 4302, (7600) Mar del Plata, Argentina

Received 13 June 1996; accepted 27 December 1996

ABSTRACT: Changes in the physical and mechanical behavior induced by two sterilization methods, gamma irradiation and ethylene oxide, were determined on two commercial medical-grade segmented polyurethanes. The two materials have different chemical composition: one is an aromatic poly(ether urethane urea), Biospan™, and the other an aliphatic ether-free polyurethane, Chronoflex™. Properties before and after sterilization procedures were compared resulting in specific structural changes for each formulation. The thermal and mechanical properties were examined using differential scanning calorimetry (DSC), dynamic mechanical analysis (DMA), stress–strain measurements, and its hysteresis cycle. Molecular weight measurements were performed by gel permeation chromatography (GPC). Sterilized Biospan samples showed a decrease in the soft-segment glass transition temperature ($T_{g,s}$) and an increase in the soft segment crystallization heat along the quenching process. Sterilized Chronoflex materials showed the opposite behavior. The hysteresis percent and residual strain percent increased after sterilization. The same effect was observed when irradiation dose and strain level increased. Surface analysis performed by scanning electron microscopy showed magnification of original surface defects after sterilization. © 1997 John Wiley & Sons, Inc. J Appl Polym Sci **65:** 1193–1203, 1997

Key words: mechanical properties; segmented polyurethanes; biomedical polyurethanes; sterilization; irradiation

INTRODUCTION

Segmented polyurethanes (SPU) have found a wide range of biomedical applications because of their appealing combination of physical and chemical properties coupled with their biocompatibility. Due to their outstanding blood-contacting performance, coupled with excellent mechanical properties, these materials became the choice for a wide variety of biomedical devices.

SPU are multiblock copolymers with a distribution of hard- and soft-segment blocks. Depending on chemical composition the hard and soft phases tend to mix or to segregate due to their immiscibility, and produce a phase-mixed or phase-separated morphology of hard-segment-rich and soft-segment-rich phases which are connected through urethane linkages. The hard-segment rich phase provides physical crosslinks within the rubbery soft segment matrix.

Biomer, a poly(ether urethane urea) developed by Ethicon, Inc., was most extensively studied in the literature, being the first SPU evaluated as a biomedical material by Pierce et al.,[1] in 1967. Biomer has been used in a number of blood-contacting devices.[2–4]

Wang and Cooper[5] investigated the morphology and properties of segmented polyether polyurethane ureas, the effect of the urea linkage, hard-segment content and block length on the ex-

Correspondence to: G. A. Abraham.

tent of phase separation, and domain structure. Furthermore, infrared studies of hydrogen bonding in SPU elastomers has been reported by Seymour, Estes, and Cooper[6] and Coleman et al.[7] Physicochemical characterization of cast and extruded Biomer has been presented by Lelah et al.[8] and several studies dealing with *in vitro* surface degradation[9–11] and *in vivo* degradation[12] are available.

However, in 1992 several suppliers decided to discontinue the manufacture and sale of some medical-grade polyurethanes, trying to avoid the potential liability costs such as those confronted by the producers of silicone raw materials.[13] After the withdrawal of traditional SPU, new medical-grade formulations were approved by the Food and Drug Administration (FDA), for the future manufacture of blood-contacting devices.

For sterilization purposes, several chemical and physical procedures can be chosen. γ-Irradiation with a dose of 2.5 Mrad has been found to be suitable to sterilize bulk materials for biomedical applications. The only disadvantage is that irradiation of polymers results in either crosslinking or chain scission, depending on the chemical nature of the polymer and irradiation dose. Electron beam radiation is effective in sterilizing surfaces and thin walled materials. Ethylene oxide gas treatment (EtO) has been successfully used as a bactericide, active at temperatures as low as 60°C. However, when EtO is used for sterilization purposes, the presence of residual EtO may result in cytotoxic action toward cells or tissues after implantation. EtO is readily absorbed by many polymers and it is not always easily desorbed. EtO molecules can interact with the urethane and urea groups through alkylating reactions, which can modify the hydrogen bonding interactions, and consequently thermal and mechanical properties.

There is no universal answer to the question of which process should be used to sterilize medical devices, because it depends on the particular composition of each material. A considerable research effort has been directed toward understanding radiation effects on polymer properties after exposure to extremely high doses,[14,15] but only a few studies are available concerning the effects of the radiation dose or the EtO used in sterilization of biomedical polymers.[16,17]

The goal of this article is to investigate the changes in physical and mechanical behavior induced by γ-irradiation (2.5 Mrad and 5.0 Mrad γ-irradiation) and EtO, on two commercially available medical-grade SPU of appreciable different chemical composition.

MATERIALS

The materials investigated were two solution-grade polyurethanes in *N,N*-dimethylacetamide (DMAc) consisting of 25% solids by weight. (1) BIOSPAN™ (The Polymer Technology Group, USA), is a segmented poly(ether urethane urea) derived from a linear block copolymer of 4,4′-diphenylmethane diisocyanate (MDI) extended with a mixture of ethylene diamine (ED) and 1,3-cyclohexanediamine, and poly(tetramethylene oxide) glycol (PTMO). The composition of Biospan was reported to be similar to Biomer™ (Ethicon, Inc., USA).[18] The chain-extended MDI is referred to as the aromatic hard segment and PTMO is referred to as the soft segment; this polymer contained as additive a linear copolymer of diisopropylaminoethyl methacrylate and decyl methacrylate 5% w/w based on dry polymer. (2) CHRONOFLEX AR™ (PolyMedica Industries, Inc., USA) is a polyurethane-polycarbonate of 4,4′-dicyclohexylmethane diisocyanate (HMDI) chain extended with 1,4-butane-diol (BD) and polycarbonate-diol. It has an aliphatic hard segment of chain-extended HMDI and soft segment of polycarbonate oxide. Chronoflex is an ether-free polyurethane.[19]

METHODS

Sample Preparation

Polymer films for physical and mechanical testing were prepared by solvent casting from DMAc solutions at 45°C on a smooth silicone rubber surface (one component, CF 1-6604, Nusil Technology, USA). The films were dried under vacuum at 60°C for 24 h in a convection oven to eliminate the last traces of solvent, cleaned in an ultrasonic bath with a Sparkleen detergent in bidistilled water, and then dried under vacuum at 60°C for 12 h. Subsequently, they were stored in a vacuum desiccator. The thicknesses of films were measured using a ultrasonic gauge Panametrics model 22DLHR coupled to a microscan contact transducer.

Polyurethane tubes were prepared in the same way as films, but instead of being solvent-casted, a 4.0 mm-diameter silicone-coated steel rod was

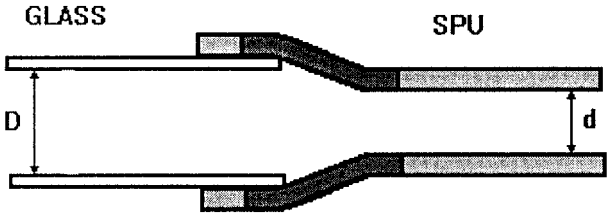

Figure 1 SPU tube coupled to glass tube.

dipped into DMAc solutions. Every tube was coupled with a 6.0 mm diameter glass rod leaving a region under stress (dark area of SPU in Fig. 1), and then placed in a dry atmosphere at room temperature. Some tubes were thermally treated for 2 h at 140°C, a temperature higher than glass transition temperature of hard segments to avoid the stressed area above mentioned.

Sterilization Procedures

Films were sealed in polyethylene bags and were exposed to 2.5 Mrad (25 KGy) or 5.0 Mrad (50 KGy) γ-irradiation ^{60}Co source. After γ-irradiation the actual dose received was measured by chemical dosimetry. The maximum values were 3.76 Mrad and 6.16 Mrad, respectively. The latter value is equivalent to the one used for re-sterilized films.

Ethylene oxide gas treatment was performed using a standard EtO sterilization apparatus (601 Hoguer Medical Industries, model 95). The samples were exposed to an atmosphere having a concentration of 310 mg/L of EtO for 4 h at 55°C. Biological indicators of *Bacillus subtilis* var. *Niger* were placed within each package as monitors of sterilization. After three vacuum cycles the chamber was aerated at atmospheric pressure for at least 48 h to remove residual EtO. Nonsterilized films were used as blank materials.

The nomenclature used is as follows: the prefix Bio- or Chro- indicates the starting material, and the suffix O, 2.5, 5, or EtO means original, 2.5 Mrad γ-irrad., 5.0 Mrad γ-Irrad., and ethylene oxide, respectively.

Infrared Spectroscopy

Transmission FTIR spectra were performed using a Bruker IFS25 spectrometer. For original Biospan, thin films were prepared. Chronoflex was dissolved in DMF and then solvent cast onto CINa plates. The thin films were thoroughly dried under vacuum at 50°C for 48 h before spectra were collected at 2 cm^{-1} resolution. The absorbance of each functional group was normalized by using the absorbance of the asymmetric (at ν_a: 2939 cm^{-1}) and symmetric (at ν_s: 2859 cm^{-1}) CH stretching vibrations. To improve the precision of the data, both normalized absorptions were calculated and averaged for each group studied.

Gel Permeation Chromatography

GPC was performed using a Waters 510 liquid chromatograph provided with a refractometric (RI) detector and a set of ultrastyragel columns with pore sizes of 500 Å, 10^3 Å, 10^4 Å, and 10^5 Å. The flow rate of degassed THF was 1 mL/min at room temperature. Monodisperse polystyrene standards, dissolved in THF, were used to calibrate the system.

A chemical modification with an excess of trifluoroacetic anhydride was used to dissolve SPU in common solvents.[20,21] The reaction was carried out at 45°C in a 2% by weight THF solution. The excess of anhydride provided a complete conversion to *N*-fluoroacetylated polyurethanes. The mixture was refluxed until a clear solution was obtained. The complete trifluoroacetylation reaction of Biospan samples required longer times (10–12 h) than Chronoflex (4–6 h) due to the difference between the two chemical structures. The solvent was distilled off at 45°C under reduced pressure and the product was allowed to dry under vacuum to ensure complete removal of unreacted trifluoroacetic anhydride and trifluoroacetic acid formed during reaction. Solutions of N-TFA derivatives at $c = 0.375$ g/dL in THF were prepared.

Differential Scanning Calorimetry

The low-temperature range (−110°C–40°C) was scanned using a thermal analyzer (Du Pont 990) with a Du Pont 910 DSC, purged with dry nitrogen, at a heating rate of 10°C/min. Equipment calibration for heat capacity measurements was performed by using an Indium standard.

The higher temperature scans were conducted from 25°C to 320°C, using Shimadzu DSC50, at the same heating rate. Before each experiment, samples were quenched from room temperature using liquid nitrogen. The glass transition temperature was taken as the onset value of the transition.

Dynamic Mechanical Testing

A Perkin–Elmer dynamic mechanical analyzer DMA-7 was used. The tests were carried out in the temperature scan mode with a three-point bending measuring system. The applied frequency was fixed at 1 Hz. A 5-mm knife edge probe and a span length specimen platform of 5 mm was used. Scans were made from an initial temperature of −120°C to 60°C at a constant heating rate of 10°C/min, operating under a dry nitrogen purge. Samples were cut into rectangular pieces of 3.5 mm × 10.00 mm and 2–3 mm thicknesses. Information about the polyurethane structure was obtained from the loss tangent peak (tan δ).

Stress–Strain Measurements

Uniaxial stress–strain data were obtained from a 1122 Instron Tensile Machine with an extensometer for elastomers, at a crosshead speed of 50 mm/min. The samples were prepared following ASTM D638 standard recommendations.

Stress Hysteresis Measurements

Hysteresis analyses were performed in a 4476 Instron Tensile Machine at room temperature and the same type of samples and speed than for the stress–strain test. This test provides data from 50 to 400% of elongation. Each sample was submitted to increasing amounts of strain, and allowed to relax at zero load for 3 min before starting each loop. Reported data are averages of at least three tests on different samples. The percent hysteresis for a given cycle was calculated from the ratio of the area bounded by the loading–unloading curves to the total area under the loading curve.

Scanning Electron Microscopy (SEM)

Scanning electron micrographs were acquired with a JEOL-JSM-35CF microscope. All samples were vacuum dried at room temperature and coated with 60 Å of gold prior to scanning.

RESULTS AND DISCUSSION

Infrared Analysis: Original Films Characterization

The absorption bands in polyurethane systems have been reported.[9,22] In the Bio-O, the NH groups were almost completely bonded for all samples. In the carbonyl region, the peak near 1733 cm^{-1} was ascribed to free urethane carbonyls, the peak near 1703 cm^{-1} was assigned to hydrogen-bonded urethane carbonyls, the peak at 1640 cm^{-1} was due to hydrogen-bonded urea carbonyls, free urea carbonyl peak at 1695 cm^{-1} was not detected. Urethane carbonyl groups reside in the border between hard and soft segments, because they are made from the reaction of the isocyanate groups of MDI and the hydroxy groups of macroglycols. The peak at 1110 cm^{-1} was assigned to the soft segment aliphatic ether stretching.

Chronoflex shows free urethane carbonyl peak at 1733 cm^{-1}, carbonate carbonyl peak at 1743 cm^{-1}, and C—O—C stretching from carbonate and urethane at 1257 cm^{-1}.

The NH groups of Chro-O were totally bonded (the signal at 3440 cm^{-1} was absent) and 76% urethane and carbonate carbonyls groups were free.

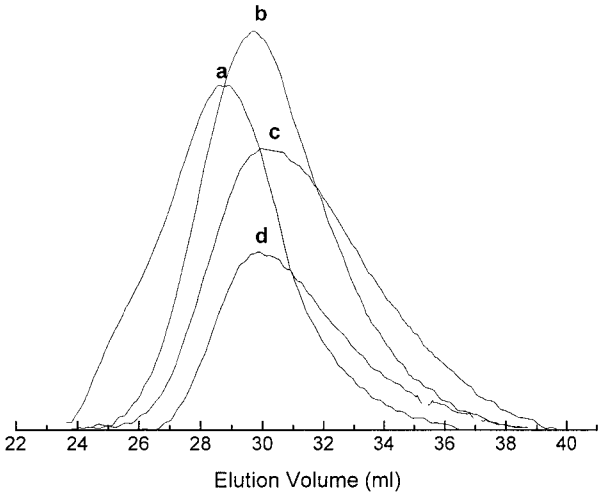

Figure 2 GPC chromatograms of Biospan series. (a) Bio-O; (b) Bio-2.5; (c) Bio-5; (d) Bio-EtO.

Gel Permeation Chromatography

The GPC chromatograms of functionalized samples showed only one peak. This indicates that the substitution degree was 100%.[21]

GPC measurements in the Biospan series evidenced that the sterilization produced a displacement to lower molecular weight from the *N*-fluoroacetylated original film as shown in Figure 2. The changes observed for the Chronoflex series

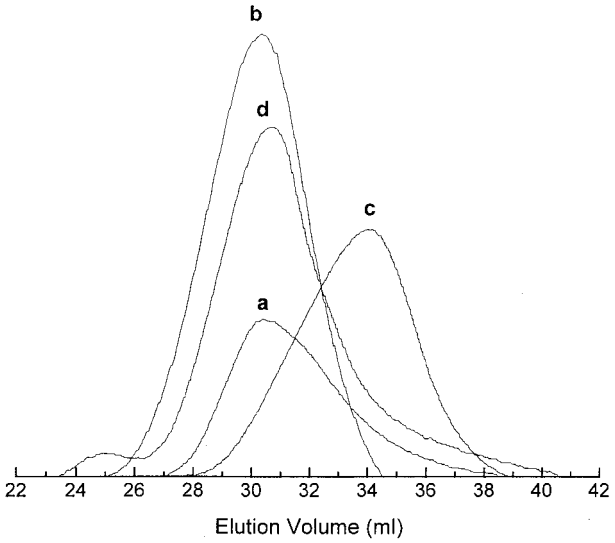

Figure 3 GPC chromatograms of Chronoflex series. (a) Chro-O; (b) Chro-2.5; (c) Chro-5; (d) Chro-EtO.

(Fig. 3) indicate a clear molecular weight decrease after irradiation with a 5 Mrad dose, but did not show any significant effects on the molecular weight distribution for the others sterilized samples. The trend observed on molecular weight suggest that some structural damage has occurred along sterilization.

Differential Scanning Calorimetry

DSC results in the low temperature range for Biospan series and Chro-O are shown in Figure 4 (first scans of quenched samples). Results for all samples are summarized in Table I. The percent crystallinity of soft-segment phases of Biospan was determined by assuming $\Delta H_{m,s}$ equal to 53 (mcal/mg) for 100% crystallinity of the PTMO-2000 homopolymer, value reported by Wang and Cooper.[5] They also founded a $T_{g,s}$ value of -79°C for the same pure homopolymer.

The DSC thermogram for nonsterilized Biospan shows the glass transition temperature of PTMO soft segments ($T_{g,s}$) at -66°C, an exothermic peak at -40°C due to the crystallization of PTMO phase, and a heat of fusion ($\Delta H_{m,s}$) of 21.9 J/g. Our experimental values compared with the values reported by Wang and Cooper for the pure homopolymer indicate a small degree of mixture between soft and hard segments, due to the relatively short hard segment length and content (22%, based on their molecular weight and mole ratio of MDI-ED-PTMO 2 : 1 : 1), which causes partial hard to soft segment intermixing as well as an isolated hard segment domain morphology. Hence, the hard segments solubilized in the soft segment matrix restrict the soft segment mobility and increase $T_{g,s}$.

The endothermic peak at 5°C was attributed to the melting of the soft segment phase, while that of the PTMO homopolymer was reported to be 24°C for metaestable crystallites and 47°C for crystallites in the equilibrium state. The lowering of the $T_{m,s}$ may be due to the small size of the microcrystalline PTMO domains.[23]

The DSC scans in the high temperature range are observed in Figure 5. The glass transition of hard domains ($T_{g,h}$) was found hardly discernible at 130°C. The endotherm at 280°C was attributed to the melting of hard segment, and it was immediately followed by the decomposition temperature. Biospan-sterilized samples showed a decrease in $T_{g,s}$ and an increase in the soft-segment crystallizing along quenching. Bio-EtO shows the highest crystallinity. This may be due to some disruption of hydrogen bonding by alkylation which produces more crystallizable soft segments.

Nonsterilized Chronoflex showed a soft-segment glass transition temperature at -32°C (Fig. 4). The hard-segment glass transition was barely detectable in the range of 120°C to 130°C (Fig. 6). The melting peak of soft segments was absent meaning that Chronoflex did not exhibit crystallizable soft segments. DSC results did not show

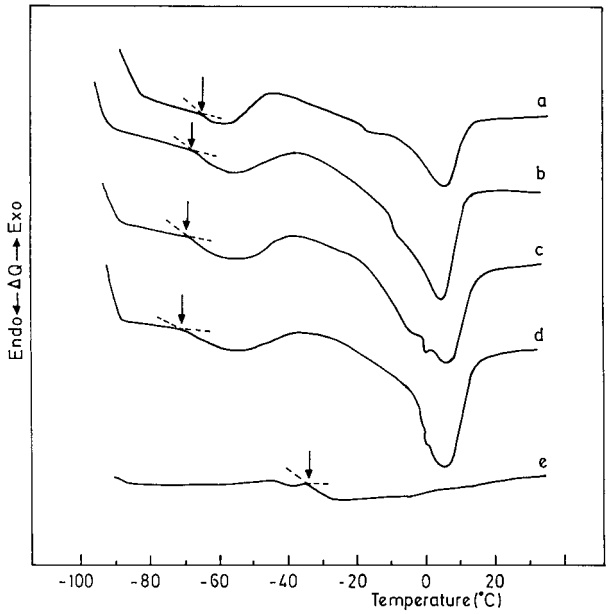

Figure 4 Low temperature DSC thermograms. (a) Bio-O; (b) Bio-2.5; (c) Bio-5; (d) Bio-EtO; (e) Chro-O.

Table I Glass Transition Temperature ($T_{g,s}$), Heat of Crystallization ($\Delta H_{c,s}$), and Heat of Crystallization along quenching ($\Delta H_{q,s}$). Melting Temperature ($T_{m,s}$), Heat of Fusion ($\Delta H_{m,s}$) and Percent of Crystallinity of Soft Segment PTMO (X_s)

Sample	$T_{g,s}$ (°C)[a]	$T_{g,s}$ (°C)[b]	$T_{m,s}$ (°C)[a]	$\Delta H_{q,s}$ (J/g)	$\Delta H_{c,s}$ (J/g)	$\Delta H_{m,s}$ (J/g)	X_s (%)
Bio-O	−66.0	−50.0	5	10.8	11.1	21.9	13.15
Bio-2.5	−69.0	−50.0	5	18.3	6.4	24.7	14.84
Bio-5	−69.0	−59.0	5	24.7	6.8	31.5	18.94
Bio-EtO	−70.0	−52.7	5	25.3	6.0	31.3	18.81
Chro-O	−32.0	−32.0	—				
Chro-2.5	−32.0	−22.6	—				
Chro-5	−32.0	−20.0	—				
Chro-EtO	−32.0	−11.7	—				

[a] Determined by DSC.
[b] Determined by DMA.

significant changes of $T_{g,s}$ values with sterilization.

Dynamic Mechanical Analysis

The dissipation factor (tan δ) of the Biospan and Chronoflex series is plotted as a function of temperature in Figures 7 and 8, respectively. Peak maxima are summarized in Table I.

The low-temperature peaks that occur at ~ -50°C for Bio-O and at −32°C for Chro-O were attributed to the soft-segment glass transitions. The differences found between the higher glass transition temperatures determined by DMA for Biospan series and the lower values determined by DSC may be attributed to the time scale of the experiment and the presence of a different fraction of crystalline segments. The presence of crystalline PTMO in DMA samples, absent in the DSC samples quenched from the melt, was ascribed to the slower cooling rate used to obtain the −120°C starting temperature in the DMA procedure (three-point bending samples are thicker than DSC ones). The higher temperature shoulder in tan δ can be associated to the increase of the crystalline fraction of PTMO.

The tan δ curves did not reveal the occurrence of the melting process. This may be because the viscoelasticity measurement is not as sensitive for detecting the melting of microcrystalline domains of PTMO in comparison with the DSC measurement.[23]

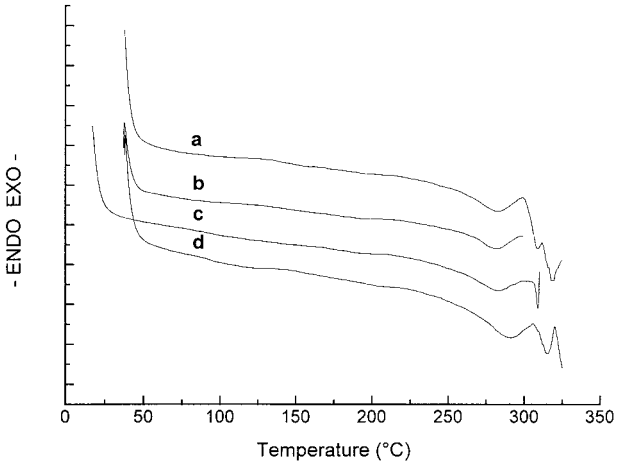

Figure 5 High temperature DSC thermograms for Biospan series. (a) Bio-O; (b) Bio-2.5; (c) Bio-5; (d) Bio-EtO.

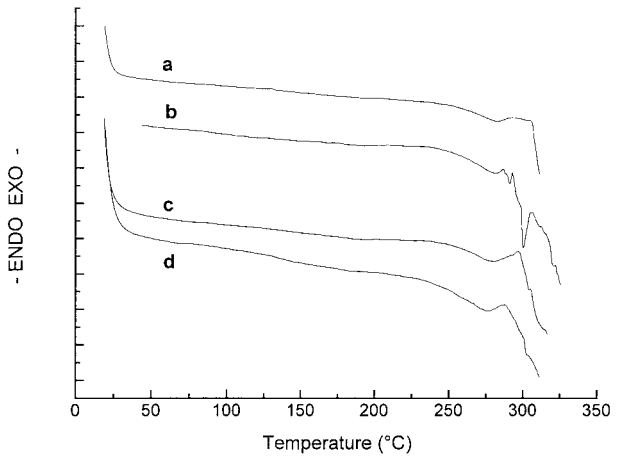

Figure 6 High temperature DSC thermograms for Chronoflex series. (a) Chro-O; (b) Chro-2.5; (c) Chro-5; (d) Chro-EtO.

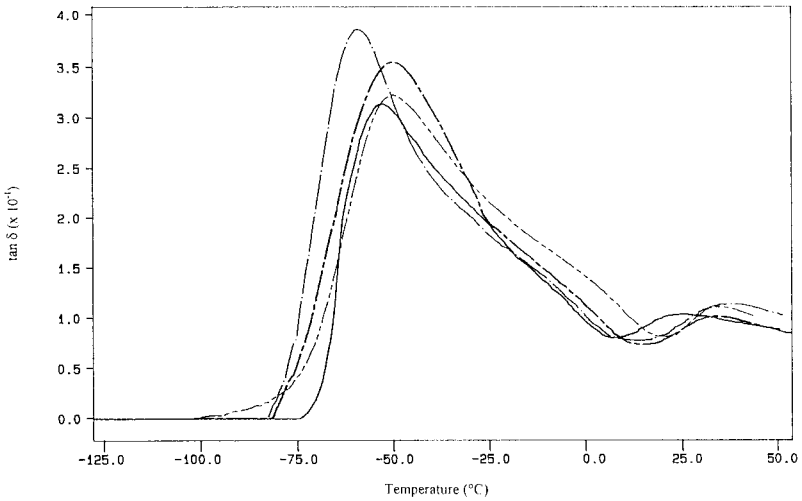

Figure 7 Dissipation factor (tan δ) versus temperature for Biospan series. Bio-O (— – – —); Bio-2.5 (— – —); Bio-5 (— · —); Bio-EtO (——).

The additional relaxation peak in the tan δ curve at $\sim$ 35°C exhibited by Biospan has been attributed to a polymethacrylate additive.[24] Other studies of this additive have been reported.[25,26]

As shown in Figures 7 and 8, after 5.0 Mrad γ-irradiation and EtO sterilization, Biospan exhibited a lower soft segment $T_{g,s}$. The opposite behavior was found for Chronoflex. The carbonate group has a much larger cohesive energy and the possibility of forming a stronger hydrogen bond with urethane group than the ether group. This promotes mixing between soft and hard segments. The increase of Chronoflex $T_{g,s}$ values may be due to the increase of mixing caused by the molecular weight decrease as result of chain scission.

The EtO treatment seems to affect the additive, showing a decrease in the temperature of tan δ peak associated to it.

Tensile Properties

The tensile properties of thermoplastic elastomers generally depends on the size, shape and concentration of hard domains, intermolecular bonding within hard domains and the ability of soft segments to crystallize under strain. Figure 9 shows the ultimate stress (σ_u), while Figure 10 shows the elongation at failure (ε%) of the Biospan and Chronoflex series.

The high tensile strength of the Biospan series

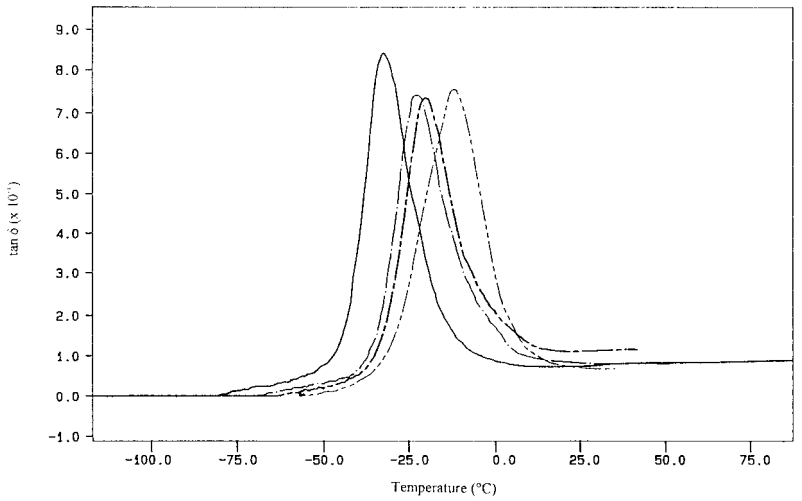

Figure 8 Dissipation factor (tan δ) versus temperature for Chronoflex series. Chro-O (——); Chro-2.5 (— · —); Chro-5 (— – —); Chro-EtO (— – – —).

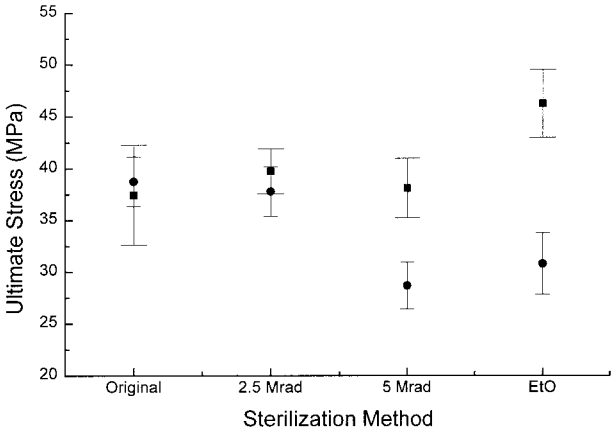

Figure 9 Ultimate stress behavior for Biospan (■) and Chronoflex (●) series.

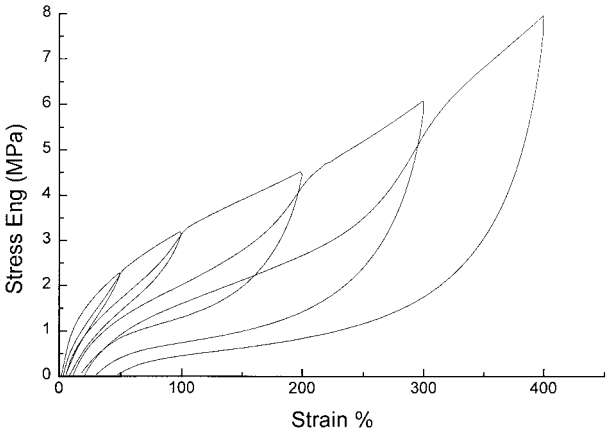

Figure 11 Stress-strain hysteresis in original Biospan.

compared with the Chronoflex series is consistent with their higher urea content, which results in more cohesive hard domains.[27] The presence of urea linkages substantially enhances the phase separation consistent with the lower $T_{g,s}$ values. Bio-EtO showed higher ultimate stress values than other samples; this may be due to stress-induced crystallization,[28] an explanation which is in agreement with the presence of more free soft segments arising from the disruption of hydrogen bridges.

Both Biospan and Chronoflex samples did not show any significant changes in secant moduli at 50% of elongation and in the values of elongation at failure. However, EtO sterilized samples displayed lower values of the latter parameter consistent with visual observations which reveal long extent of stress whitening due to crystallization of free soft segments produced by chain scission.

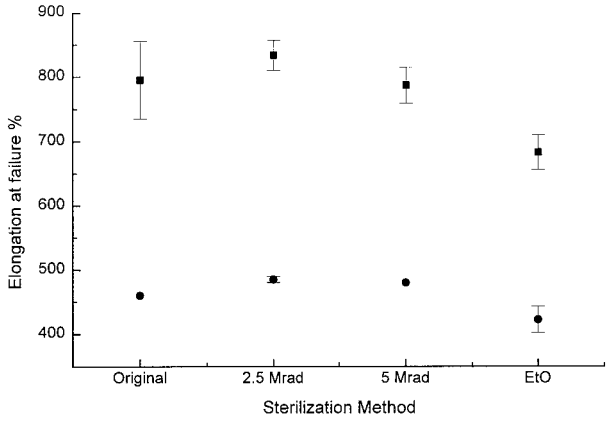

Figure 10 Elongation at failure behavior for Biospan (■) and Chronoflex (●) series.

Stress Hysteresis Studies

In a multiphase system, the stress hysteresis behavior is closely related to the domain morphology and the phase separation degree.[29,30] Hysteresis was also reported to be composition dependent, so elastomeric properties preferably were obtained for samples containing isolated hard segment domains (25% hard segment).[31]

Different mechanisms may be responsible for hysteresis losses at different elongations. The stress-hysteresis is attributed to a yielding-like disruption of the system of hydrogen bridges in the hard-segment regions with strain, leading to a decrease in reinforcement of the rubbery phase upon strain cycling and promoting a permanent deformation.

Figure 11 shows typical stress hysteresis cycles obtained with nonsterilized Biospan samples. The hysteresis percent as a function of strain is shown in Figure 12 for all materials.

The Biospan series initially shows a low hysteresis, consistent with a morphology of isolated hard domains dispersed in an amorphous soft segment matrix. At low elongations, i.e., $<50\%$, the rather high level of energy dissipation was associated with a non-affine deformation and a minimal orientation of hard segment domains.[31] After a 100% strain level, hysteresis traces exhibit a rising rate trend with the increasing strain level. The latter result suggests some partial disruption of soft segment domains, alignment of hard segments into the stretch direction and even the possibility of some irreversible strain-induced crystallization at higher extension ratios.

The residual strain percent followed the same

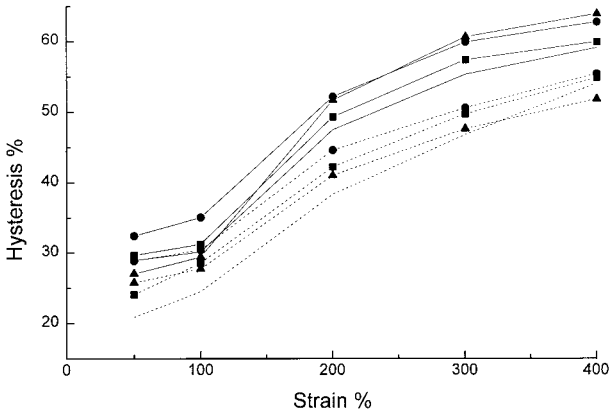

Figure 12 Hysteresis behavior versus elongation curves. Biospan series: Bio-O (——); Bio-2.5 (— ■ —); Bio-5 (— ● —); Bio-EtO (— ▲ —). Chronoflex series: Chro-O (· · · · ·); Chro-2.5 (· · ·■· · ·); Chro-5 (· · ·●· · ·); Chro-EtO (· · ·▲· · ·).

patterns displayed by the hysteresis curves (Figs. 13 and 14).

The hysteresis percent and residual strain percent increased after sterilization. The same effect was observed when the irradiation dose and the strain level increased.

SEM Studies

Wu et al.[32] found that the amphiphilic additive Methacrol 2138F (similar to the additive reported for Biospan)[18] is phase-separated as discrete domain structures, ~ 0.5 μm in diameter. This additive can be regarded as a polymeric surfactant in the sense that it is enriched at the polymer/air interface, decreasing the interfacial free energy

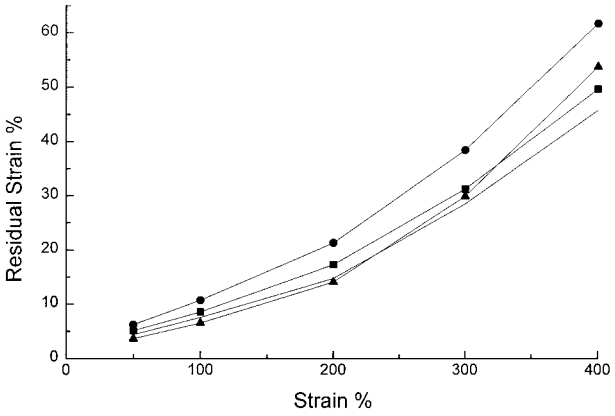

Figure 13 Residual strain as a function of elongation for Biospan series. Bio-O (——); Bio-2.5 (— ■ —); Bio-5 (— ● —); Bio-EtO (— ▲ —).

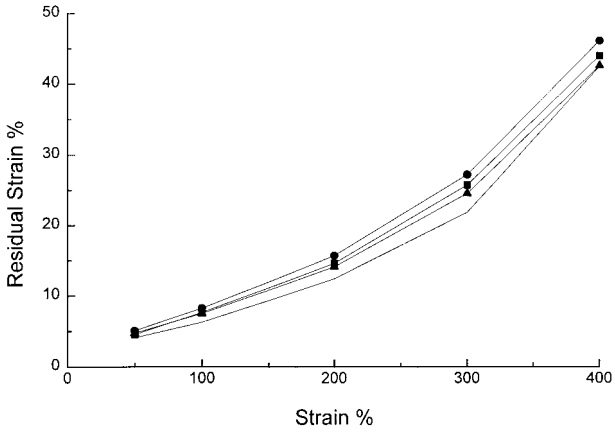

Figure 14 Residual strain as a function of elongation for Chronoflex series. Chro-O (——); Chro-2.5 (— ■ —); Chro-5 (— ● —); Chro-EtO (— ▲ —).

by introducing long alkyl chains of low polarity in the interface. The formation of small pits about 5 μm diameter after implantation was previously assigned to the leaching out of the additive present at the surface.[12,24] Santowhite Powder was also reported by Wu et al.[32] to be present in Biomer as an effective inhibitor surface cracking.

SEM micrographs of Biospan series are shown in Figure 15. The lack of evidence of microcraking in Biospan samples, may be due to the presence of an antioxidant. However, the surface of Bio-EtO shows some microcraks. Extensive pitting is also observed in Biospan series. The number and size of pits were highest in Bio-EtO and decreased from Bio-5 to Bio-2.5 samples. Magnification of original surface defects after sterilization was found for all samples. Then the generation of surface defects should be minimized by controlling the solution-casting process conditions.

In the case of Chronoflex samples, the surface appeared not affected by sterilization methods. In both materials, the level of stress applied did not introduce differences on surface appearance between performed tubes and those having a coupled area under stress.

CONCLUSIONS

The sterilization process introduces specific structural and surface changes in polyurethane formulations. The damage could be detected by the molecular weight decrease, the soft segment crystallinity increase after quenching, and the increase in hysteresis and residual stress values.

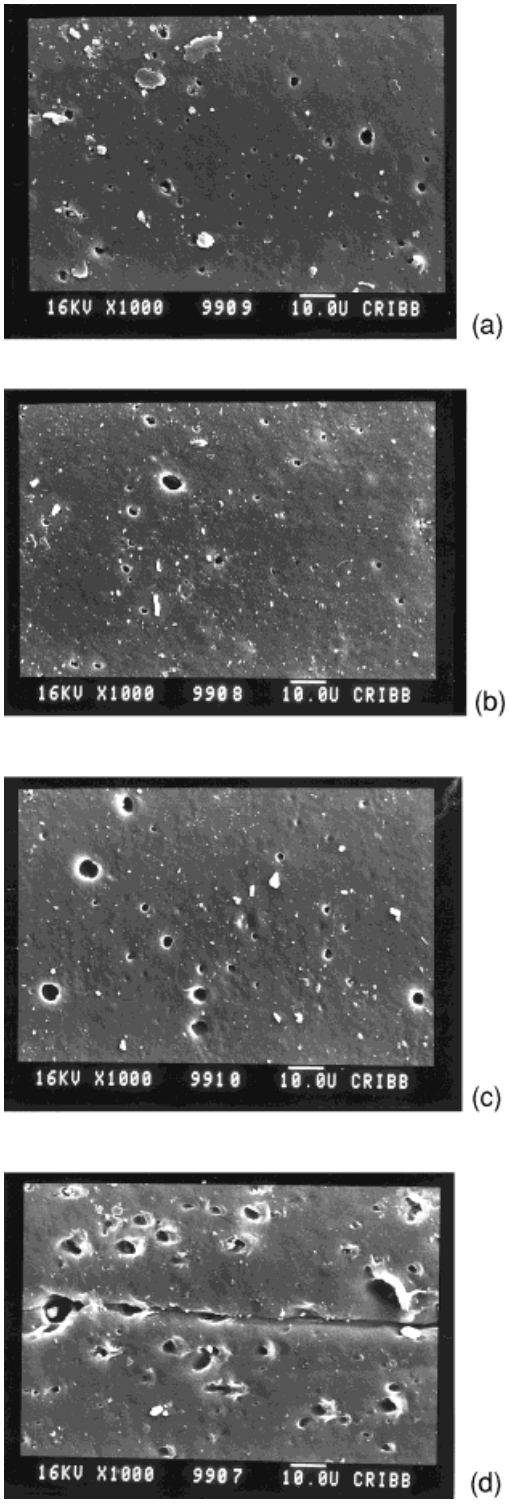

Figure 15 SEM micrographs of Biospan series. (a) Bio-O; (b) Bio-2.5; (c) Bio-5; (d) Bio-EtO.

The damage appears when the general irradiation dose of 2.5 Mrad is applied and they increase at higher γ-irradiation doses. EtO sterilized samples showed a significative decrease of the elongation at failure. Bio-EtO sample showed a higher ultimate stress.

The opposite trend in $T_{g,s}$ values determined by DMA of two commercial formulations is a result of their different chemical composition.

The prior device contamination and the particular materials composition should be taken into account when selecting the appropriate sterilization method.

All Biospan samples analyzed by SEM showed a magnification of original surface defects after sterilization, whereas the surface of Chronoflex did not appear affected by sterilization. The generation of surface defects and the bioburden should be minimized by controlling the solution-casting process conditions and the device assembling procedures.

This work was supported by the National Research Council, Argentina (CONICET). G. Abraham thanks CONICET for the fellowship awarded. The authors thank Dra. N. Kaupert (National Commission of Atomic Energy, Ezeiza), Liliana Di Lorenzo from Community Hospital of Mar del Plata for sample sterilizations, and Diana Fasce from INTEMA for FTIR and GPC measurements.

REFERENCES

1. W. S. Pierce, M. C. Turner, J. W. Boretos, H. D. Metz, S. P. Nolan, and A. G. Morrow, *Trans. ASAIO,* **13,** 299 (1967).
2. J. W. Boretos, W. S. Pierce, R. E. Baier, A. F. LeRoy, and H. J. Donachy, *J. Biomed. Mater. Res.,* **9,** 327 (1975).
3. T. Kolff, G. Burkett, and J. Feyen, *Biomat. Med. Dev., Artif. Organs,* **1**(4), 669 (1973).
4. J. W. Boretos, *Pure Appl. Chem.,* **52,** 1851 (1980).
5. C. B. Wang and S. L. Cooper, *Macromolecules,* **16,** 775 (1983).
6. R. W. Seymour, G. M. Estes, and S. L. Cooper, *Macromolecules,* **3,** 579 (1970).
7. M. C. Coleman, D. J. Skrovanek, J. Hu, and P. C. Painter, *Macromolecules,* **21,** 59 (1988).
8. M. D. Lelah, L. K. Lambrecht, B. R. Young, and S. L. Cooper, *J. Biomed. Mater. Res.,* **17,** 1 (1983).
9. R. E. Marchant, Q. Zhao, J. M. Anderson, and A. Hiltner, *Polymer,* **28,** 2032 (1987).
10. R. E. Marchant, Q. Zhao, J. M. Anderson, A. Hiltner, and R. S. Ward, in *Surface Characterization of Biomaterials,* B. D. Ratner, Ed., Elsevier, Amsterdam (1988).
11. G. F. Meijs, S. J. McCarthy, E. Rizzardo, Y. Chen,

R. C. Chatelier, A. Brandwood, and K. Schindhelm, *J. Biomed. Mat. Res.,* **27,** 345 (1993).
12. Y. Wu, C. Sellitti, J. M. Anderson, A. Hiltner, G. A. Lodoen, and C. R. Payet, *J. Appl. Polym. Sci.,* **46,** 201 (1992).
13. M. Szycher, A. Siciliano, and A. Reed, in *Polymeric Biomaterials,* S. Dumitriu, Ed., Marcel Dekker, New York, 1994, Chapter 6.
14. N. Martakis, M. Niaounakis, and D. Pissimissis, *J. Appl. Polym. Sci.,* **51,** 313 (1994).
15. M. Deng and S. W. Shalaby, *J. Appl. Polym. Sci.,* **58,** 2111 (1995).
16. M. Szycher, in *Blood Compatible Materials and Devices,* C. P. Sharma and M. Szycher, Eds., Technomic, Lancaster, 1991, Chap. 5.
17. S. Dumitriu and C. Dumitriu-Medvichi, in *Polymeric Biomaterials,* S. Dumitriu, Ed., Marcel Dekker, New York, 1994, Chap. 1.
18. The Polymer Technology Group, Inc. Emeryville, CA, Products Information.
19. PolyMedica Industries, Inc., Golden, CO, Products Information.
20. E. W. Merrill and N. A. Mahmud, *Polym. Comm.,* **26,** 105 (1985).
21. E. Biagini, E. Gattiglia, E. Pedemonte, and S. Russo, *Makromol. Chem.,* **184,** 1213 (1983).
22. M. D. Lelah and S. L. Cooper, in *Polyurethanes in Medicine,* C.R.C. Press, Florida, 1989, Chap. 7.
23. T. Takigawa, M. Oodate, K. Urayama, and T. Masuda, *J. Appl. Polym. Sci.,* **59,** 1563 (1996).
24. C. Freij-Larsson, M. Kober, B. Wesllén, E. Willquist, and P. Tengvall, *J. Appl. Polym. Sci.,* **49,** 815 (1993).
25. M. Brunstedt, N. P. Ziats, M. Schubert, P. A. Hiltner, J. M. Anderson, G. A. Lodoen, and C. R. Payet, *J. Biomed. Mater. Res.,* **27,** 255 (1993).
26. M. Brunstedt, N. P. Ziats, S. Robertson, A. Hiltner, J. M. Anderson, G. A. Lodoen, and C. R. Payet, *J. Biomed. Mater. Res.,* **27,** 367 (1993).
27. T. O. Ahn, S. Jung, H. M. Jeong, and S. W. Lee, *J. Appl. Polym. Sci.,* **51,** 43 (1994).
28. L. Morbitzer and H. Hespe, *J. Appl. Polym. Sci.,* **16,** 2697 (1972).
29. C. S. P. Sung, T. W. Smith, and N. H. Sung, *Macromolecules,* **13,** 117 (1980).
30. R. W. Seymour, A. E. Jr. Allegrezza, and S. L. Cooper, *Macromolecules,* **6,** 896 (1973).
31. S. Abouzahr, G. L. Wilkes, and Z. Ophir, *Polymer,* **23,** 1077 (1982).
32. Y. Wu, Q. Zhao, J. M. Anderson, A. Hiltner, G. A. Lodoen, and C. R. Payet, *J. Biomed. Mater. Res.,* **25,** 725 (1991).